IPR – INSTITUT DE PRODUCTION & ROBOTIQUE
LABORATOIRE DE PRODUCTION MICROTECHNIQUE (LPM)
Thomas Maeder
CH-1015 LAUSANNE, Switzerland
☎: + 41 21 693 58 23
Fax : + 41 21 693 38 91
thomas.maeder@epfl.ch
http://ipr.epfl.ch

ÉCOLE POLYTECHNIQUE
FÉDÉRALE DE LAUSANNE

2003-05-22 contraintes joint brasé poutre-embase MilliNewton.docx

Stress distribution in cantilever – base joints

Estimation of the stress distribution in the solder or glue joint between a cantilever and its base, and of the corresponding bending stress distribution in the cantilever.

Estimation de la distribution de contraintes dans un joint collé ou brasé entre un cantilever et sa base, et de distribution correspondante de la contrainte en flexion dans le cantilever.

Einschätzung der Spannungsverteilung in einem geklebten oder geloteten Gefüge zwischen einem Biegebalken und seiner Unterlage, und der entsprechenden Verteilung der Biegespannung im Balken.

Thomas Maeder, 13.5.2003

Project: MilliNewton

Keywords: force sensor, pressure sensor, cantilever, resonance, solder, glue.

Table of contents

Summary

This reports details results of modelling of the stresses in the solder or glue joints linking a cantilever to its base, using analytical and finite difference methods. The additional compliance due to joint deformation and its effect on the resonance frequency is also calculated.

The parameters used in the examples are those of the MilliNewton force sensor (the three force ranges). Additionally, the effect of variations of joint length and joint elastic modulus (solder or glue) are studied and discussed. Also, the effect of introducing a yield stress for the joint material (valid especially for solder) is examined.

Finally, the model is applied to previous solder strength studies and to the case of glass sealing.

1. Introduction

Cantilever-type thick-film piezoresistive force sensors assembled by gluing or soldering a cantilever force cell onto a base are simple products compatible with inexpensive mass production. In the case or solder (or conductive glue), the mechanical assembly can also act as an electrical link, obviating the need for an additional connexion step such as wire bonding.

However, this geometry does have some problems, due to the behaviour of the glue or solder. These materials are not well defined mechanically, as they can exhibit viscoelastic / viscoplastic behaviour, which produces parasitic stresses in the cantilever that evolve over time, causing drift of the output signal. Moreover, the joints usually have some porosity, which affects the stress distribution.

The strength of solder joints can be surprisingly high, as observed by Sven Stauss[i]. This is probably due to clamping of the solder by the substrate, which tends to suppress plastic deformation.

This work aims to calculate the macroscopic stress distribution, using the simplified model outlined below:

- The cantilever has a constant rectangular cross-section and deforms only by bending.
- The base is infinitely rigid.
- The joint has a constant thickness and the same width as the cantilever beam. It deforms only vertically, according to two constant materials properties: its (effective) elastic modulus and yield strength.
- Edge effects (sideways and at the ends of the joint) are ignored.

2. Description of the model

The parameters of the model are schematised in fig. 1, and described in table 1. The x and y coordinate axes are also given in fig. 1. The origin for x is the end of the joint, with the free cantilever for $x > 0$ and the joint for $x < 0$. The origin for y corresponds to zero displacement of the cantilever.

In this model, it is assumed that the cantilever and the joint have a rectangular cross section, and share the same width b.

Stresses and strains are defined positive in tension and negative in compression. The bending stress given for the cantilever is the stress in the top side.

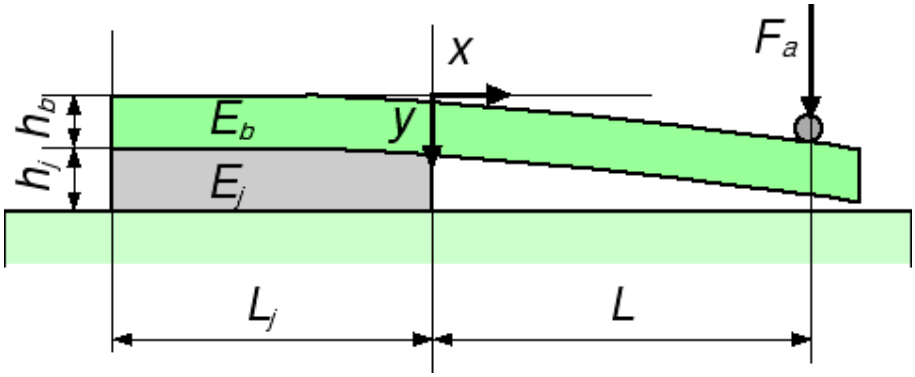

Figure 1. Parameters of the model and coordinate axes.

Symbol	Description
E_b	Cantilever effective elastic modulus
h_b	Cantilever thickness
E_j	Joint elastic modulus
h_j	Joint thickness
L_j	Joint length
L	Cantilever effective length
F_a	Applied bending force
b	Width of cantilever and of joint

Table 1. Parameters of the model.

3. Analytical treatment

3.1. Differential equation for displacement

We first define the moment of inertia I and strength W in bending for a cantilever beam of rectangular cross-section, which are constant throughout the length.

(1) $$I = \frac{b \cdot h_b^3}{12} \text{ and } W = \frac{b \cdot h_b^2}{6}$$

The bending moment $M(x)$ and the bending stress $\sigma_b(x)$ in the cantilever are determined by the curvature of the beam $y''(x)$, which is the 2nd derivative of the displacement $y(x)$:

(2) $$M = E_b \cdot I \cdot y''$$

(3) $$\sigma_b = E_b \cdot \frac{I}{W} \cdot y'' = E_b \cdot \frac{h_b}{2} \cdot y''$$

The force $F(x)$ carried by the cantilever is the (opposite in our coordinate system) derivative of the bending moment, and is therefore a function of the 3rd derivative of y:

(4) $$F = -M' = -E_b \cdot I \cdot y'''$$

The above equations are valid throughout the length of the beam. The derivative of F is zero in the effective length domain ($0 < x < L$). In the joint ($-L_j < x < 0$), it is determined by the stress $\sigma_j(x)$ in the joint:

(5) $$F' = -b \cdot \sigma_j$$

To "close the circle" and thereby get a differential equation for y, we must link σ_j to y. This is done through the strain $\varepsilon_j(x)$, which is determined by σ_j. Therefore, the displacement y is defined by the following set of equations:

(6) $$\sigma_j = -\frac{F'}{b} = +\frac{M''}{b}$$

(7) $$y = -h_j \cdot \varepsilon_j\left(\sigma_j\right)$$

If we assume the behaviour of the joint to be purely elastic, we get a simple 4th-order differential equation for y:

(8) $$\sigma_j = E_j \cdot \varepsilon_j$$

(9) $$y = -\frac{E_b \cdot I \cdot h_j}{E_j \cdot b} \cdot y'''' = -\frac{E_b \cdot h_b^3 \cdot h_j}{12 E_j} \cdot y''''$$

2.2. Solution of the differential equation for elastic case

Equation (9) is of the linear homogeneous type[ii]. The general solution is given by:

(10) $$y = \exp\left(+\frac{x}{L_c}\right) \cdot \left[A \cdot \cos\left(\frac{x}{L_c}\right) + B \cdot \sin\left(\frac{x}{L_c}\right)\right] + \exp\left(-\frac{x}{L_c}\right) \cdot \left[C \cdot \cos\left(\frac{x}{L_c}\right) + D \cdot \sin\left(\frac{x}{L_c}\right)\right]$$

The coefficients A, B, C and D are determined by the boundary conditions, and L_c is the "caracteristic length", given by:

(11) $$L_c = \left(\frac{4 E_b \cdot I \cdot h_j}{E_j \cdot b}\right)^{\frac{1}{4}} = \left(\frac{E_b \cdot h_b^3 \cdot h_j}{3 E_j}\right)^{\frac{1}{4}}$$

The physical meaning of L_c is the decay length of the stress in the joint as one moves away from the load-carrying end. It is a "competition" between the bending stiffness of the beam, given by term $E_b I$, and the compression / tension stiffness of the joint, given by term $E_j b/h_j$.

- A stiff cantilever and a soft joint give large L_c values, e.g. a thick cantilever with glue.
- A compliant cantilever and a hard joint give small L_c values, e.g. a thin membrane with a glass seal.

The derivatives of (10) are given below. We easily verify that expressions (10) and (15) satisfy the differential equation (9).

$$(12)\quad L_c \cdot y' = \exp\left(+\frac{x}{L_c}\right)\cdot\left[(A+B)\cdot\cos\left(\frac{x}{L_c}\right)+(B-A)\cdot\sin\left(\frac{x}{L_c}\right)\right] + \exp\left(-\frac{x}{L_c}\right)\cdot\left[(D-C)\cdot\cos\left(\frac{x}{L_c}\right)-(C+D)\cdot\sin\left(\frac{x}{L_c}\right)\right]$$

$$(13)\quad \frac{L_c^2}{2}\cdot y'' = \exp\left(+\frac{x}{L_c}\right)\cdot\left[B\cdot\cos\left(\frac{x}{L_c}\right)-A\cdot\sin\left(\frac{x}{L_c}\right)\right] + \exp\left(-\frac{x}{L_c}\right)\cdot\left[-D\cdot\cos\left(\frac{x}{L_c}\right)+C\cdot\sin\left(\frac{x}{L_c}\right)\right]$$

$$(14)\quad \frac{L_c^3}{2}\cdot y''' = \exp\left(+\frac{x}{L_c}\right)\cdot\left[(B-A)\cdot\cos\left(\frac{x}{L_c}\right)-(A+B)\cdot\sin\left(\frac{x}{L_c}\right)\right] + \exp\left(-\frac{x}{L_c}\right)\cdot\left[(C+D)\cdot\cos\left(\frac{x}{L_c}\right)+(D-C)\cdot\sin\left(\frac{x}{L_c}\right)\right]$$

$$(15)\quad -\frac{L_c^4}{4}\cdot y'''' = \exp\left(+\frac{x}{L_c}\right)\cdot\left[A\cdot\cos\left(\frac{x}{L_c}\right)B\cdot\sin\left(\frac{x}{L_c}\right)\right] + \exp\left(-\frac{x}{L_c}\right)\cdot\left[C\cdot\cos\left(\frac{x}{L_c}\right)+D\cdot\sin\left(\frac{x}{L_c}\right)\right]$$

2.3. Boundary conditions

The four boundary conditions which must be satisfied are given by the force F and bending moment M, at both ends of the joint. Note that these are valid whether the joint behaves elastically or not.

$$(17)\quad F(0) = F_a$$

$$(18)\quad M(0) = F_a \cdot L$$

$$(19)\quad F\left(-L_j\right) = 0$$

$$(20)\quad M\left(-L_j\right) = 0$$

2.4. Solution for elastic case with $L_j >> L_c$

For large values of L_j, one easily verifies that equations (19) and (20) translate to $C = D = 0$. In this case, A and B are given by:

$$(21)\quad A = \frac{F_a \cdot L_c^2}{2E_b \cdot I} \cdot \left(L + L_c\right) = y(0)$$

$$(22)\quad B = \frac{F_a \cdot L \cdot L_c^2}{2E_b \cdot I}$$

The maximum absolute value of the joint stress occurs at x = 0. The stress, σ_{j0}, is negative for downward applied force.

$$(23)\quad \sigma_{j0} = -\frac{F_a \cdot L_c^2 \cdot E_j}{2E_b \cdot I \cdot h_j} \cdot \left(L + L_c\right)$$

Deformation in the joint lowers the stiffness k of the cantilever structure through the displacement and slope at x = 0. This joint stiffness k_j is given by:

$$(24)\quad k_j = \frac{F_a}{y(0) + y'(0) \cdot L} = \frac{F_a \cdot L_c}{A \cdot L_c + (A + B) \cdot L} = \frac{2E_b \cdot I}{L_c \cdot \left(2L^2 + 2L \cdot L_c + L_c^2\right)}$$

This must be combined to the stiffness k_b of the beam in flexion to give k:

$$(25)\quad k_b = \frac{3E_b \cdot I}{L^3}$$

$$(26)\quad \frac{1}{k} = \frac{1}{k_b} + \frac{1}{k_j}$$

3. Finite difference (FD) method

Solving equations (6) and (7) by the finite difference (FD) method, with a discrete mesh of element size Δx allows additional flexibility. For instance, it enables plastic deformation of a solder joint to be taken into account.

The 1st and 2nd derivatives of the displacements y_i are given by the following relations:

$$(27)\quad y'_i = \frac{y_{i+1} - y_{i-1}}{2 \cdot \Delta x}$$

$$(28)\quad y''_i = \frac{y_{i+1} - 2y_i + y_{i-1}}{\Delta x^2}$$

The bending moments M_i are calculated from y''_i according to equation (2), and y_i is calculated for the next iteration according to (6) and (7). In contrast to the analytical solution, we define a yield stress σ_e for pure plastic strain, according to fig. 2, and introduce a plastic strain ε_{jp}.

$$(29)\quad y = -h_j \cdot \varepsilon_j = -h_j \cdot \left(\frac{\sigma_j}{E_j} + \varepsilon_{jp}\right) = -h_j \cdot \left(\frac{M''}{b \cdot E_j} + \varepsilon_{jp}\right)$$

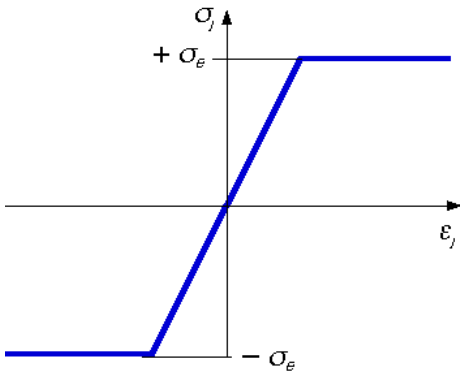

Figure 2. Assumed model for yielding of the joint material.

The 2nd derivative of the bending moment M'' is evaluated in a similar fashion to y'' according to the finite difference method:

$$(30) \quad M''_i = \frac{M_{i+1} - 2M_i + M_{i-1}}{\Delta x^2}$$

The values of y, M and ε_{jp} are obtained by an iterative process. Plastic strain is incremented or decremented after comparing the calculated joint stress with σ_e, using the model depicted in fig. 2.

4. Numeric calculations

The following calculations use the MilliNewton force sensor as a starting point, and study the effect of parameters such as joint length, cantilever thickness, joint elastic modulus (solder or glue), and joint yield stress.

4.1. Comparison of analytical & finite difference methods

The results of analytical and FD calculations ($\Delta x = 0.05$ and 0.10 mm) are compared for one set of parameters (1N MilliNewton sensor). The joint was assumed to behave elastically, and to have an elastic modulus of 30 GPa (typical for solder), and a thickness of 0.1 mm. Parameters and results are summarised in table 2, and the resulting curves are given in fig. 3.
The results show very good agreement between analytical and FD methods, even at a relatively coarse step of 0.1 mm. Also, 2.5 mm of solder (MilliNewton) is clearly long enough for this force range, as the stresses completely decay before the end of the joint.

Symbol	Description	Value	
E_b	Cantilever effective elastic modulus	330	GPa
E_j	Joint elastic modulus	30	GPa
h_b	Cantilever thickness	0.40	mm
h_j	Joint thickness	0.10	mm
L_j	Joint length (for finite difference method)	2.5 & 5.0	mm
L	Cantilever effective length	8.0	mm
b	Width of cantilever and of joint	3.0	mm
L_c	Calculated caracteristic length	0.39	mm
F_a	Applied bending force	1.0	N
σ_{j0}	Calculated stress in joint at x=0 (analytical)	-36.5	MPa
σ_{j0}	FD stress in joint at x=0 (FD, Δx = 0.05 mm)	-36.2	MPa
σ_{j0}	FD stress in joint at x=0 (FD, Δx = 0.10 mm)	-35.5	MPa

Table 2. Parameters & calculated values.

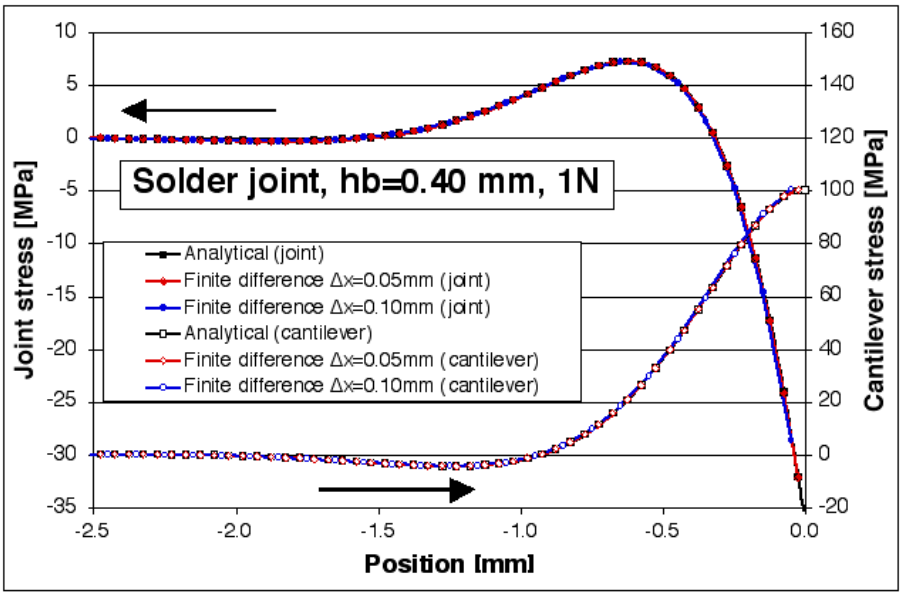

Figure 3. Stresses in cantilever & joint, by analytical & FD methods (two element sizes).

4.2. Effect of cantilever thickness, 5 mm and 2.5 mm solder joint

Results (FD) are given here for an elastic, solder joint, for the three thicknesses of the MilliNewton sensor cantilever beam (alumina material). Two lengths (2.5 mm and 5.0 mm) are studied here, 2.5 mm being the length of the main solder pad of MilliNewton. Table 4 gives the corresponding parameters and the calculated characteristic lengths and joint stresses, and the results of FD calculations are given in figures 4 and 5. For the joint thickness h_j, a "reasonable" value of 0.1 mm was chosen.

The results show that 2.5 mm of solder seem to be enough even for the thickest cantilever. However, the stress at the end of the joint is very large. Within the joint, clamping effects (see section 4.6 and discussion) would theoretically prevent plastic deformation. This is however not valid at the edges, and around pores in the joint.
The overall stiffness drops by ca. 10…20% due to deformation of the joint, which should translate into a ca. 5…10% drop in resonance frequency.

Symbol	Description	Value (400)	Value (1'000)	Value (2'000)	
E_b	Cantilever effective elastic modulus	330	330	330	GPa
E_j	Joint elastic modulus	30	30	30	GPa
h_b	Cantilever thickness	0.25	0.40	0.63	mm
h_j	Joint thickness	0.10	0.10	0.10	mm
L_j	Joint length (for finite difference method)	5.0, 2.5	5.0, 2.5	5.0, 2.5	mm
L	Cantilever effective length	8.0	8.0	8.0 mm	mm
b	Width of cantilever and of joint	3.0	3.0	3.0	mm
L_c	Calculated caracteristic length (analytical)	0.28	0.39	0.55	mm
F_a	Applied bending force	0.4	1.0	2.0	N
σ_{j0}	Calculated stress in joint at x=0 (analytical)	-29.2	-36.5	-37.7	MPa
σ_{jmax}	Calculated max. tensile stress in joint (FD)	5.8	7.2	7.3	MPa
k_b	Calculated beam stiffness	7.6	30.9	123.8	N/mm
k_j	Calculated joint stiffness	70.7	200.7	556.4	N/mm
k	Calculated overall stiffness	6.8	26.8	101.3	N/mm

Table 3. Parameters & calculated values, for the three force ranges of MilliNewton.

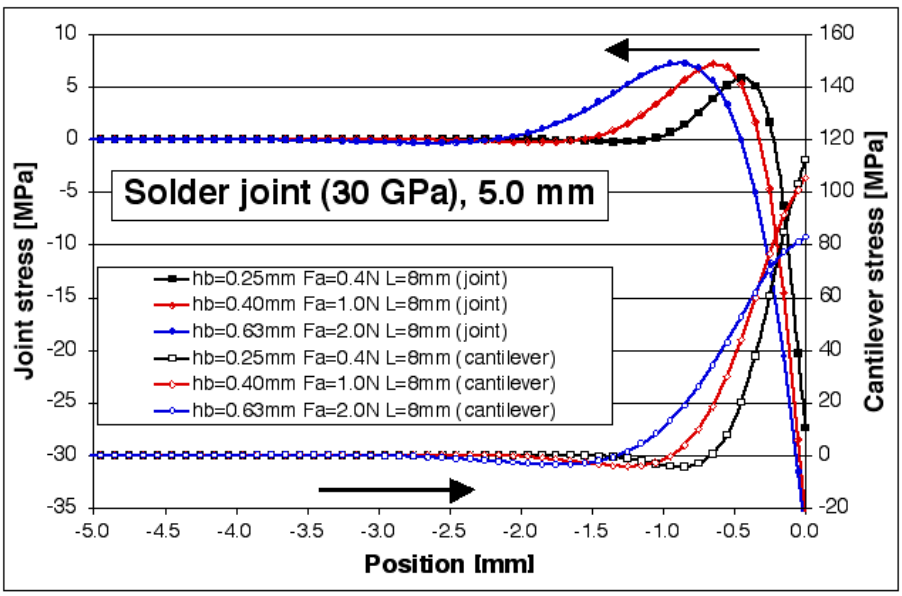

Figure 4. Stresses in cantilever & joint calculated by FD for 5.0 mm long solder joints.

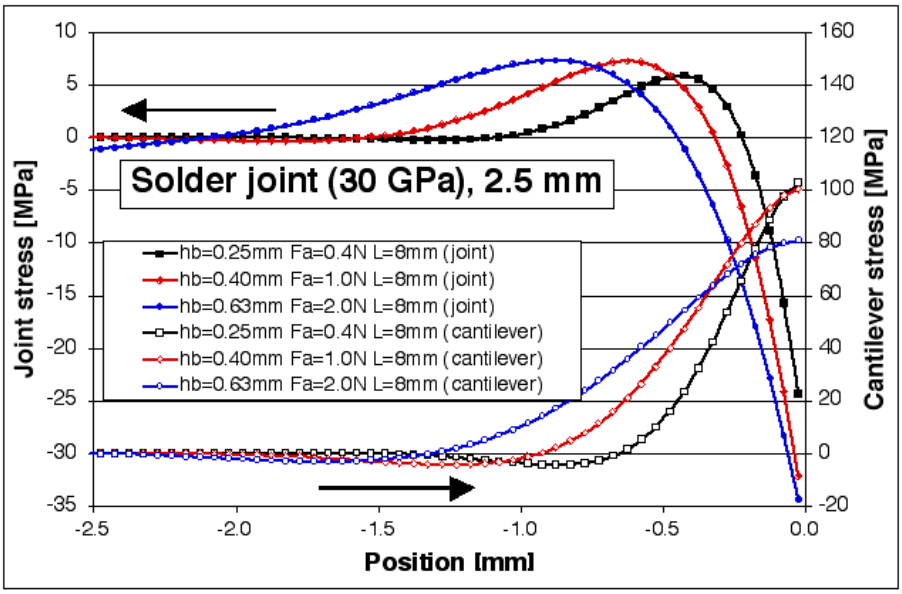

Figure 5. Stresses in cantilever & joint calculated by FD for 2.5 mm long solder joints.

4.3. Effect of replacing solder by glue

Taking the same parameters as the previous section, except replacing solder ($E_j \cong 30$ GPa) by much more compliant conductive glue ($E_j \cong 3$ GPa), results in a much longer decay length of the stresses and a higher drop in stiffness, but also in much lower stresses in the joint (table 4 and figures 6 & 7). In this case, the probable extent of plastic deformation is much less than for solder, which is favourable for drift characteristics.

Due to the higher L_c values, the stress in the joint does not decay completely throughout the joint length for the highest force range of MilliNewton (2.5 mm main joint length). However, this entails only a modest increase of maximum tensile stress: 2.6 vs. 2.3 MPa.

Symbol	Description	Value (400)	Value (1'000)	Value (2'000)	
E_b	Cantilever effective elastic modulus	330	330	330	GPa
E_j	Joint elastic modulus	3	3	3	GPa
h_b	Cantilever thickness	0.25	0.40	0.63	mm
h_j	Joint thickness	0.10	0.10	0.10	mm
L_j	Joint length (for finite difference method)	5.0, 2.5	5.0, 2.5	5.0, 2.5	mm
L	Cantilever effective length	8.0	8.0	8.0	mm
b	Width of cantilever and of joint	3.0	3.0	3.0	mm
L_c	Calculated caracteristic length (analytical)	0.49	0.70	0.98	mm
F_a	Applied bending force	0.4	1.0	2.0	N
σ_{j0}	Calculated stress in joint at x=0 (analytical)	-9.5	-12.0	-12.5	MPa
σ_{jmax}	Calculated max. tensile stress in joint (FD)	1.8	2.3	2.3, 2.6	MPa
k_b	Calculated beam stiffness	7.6	30.9	123.8	N/mm
k_j	Calculated joint stiffness (L_j = 5 mm)	38.7	108.7	296.6	N/mm
k	Calculated overall stiffness (L_j = 5 mm)	6.3	24.1	87.3	N/mm

Table 4. Parameters & calculated values, for the three force ranges of MilliNewton.

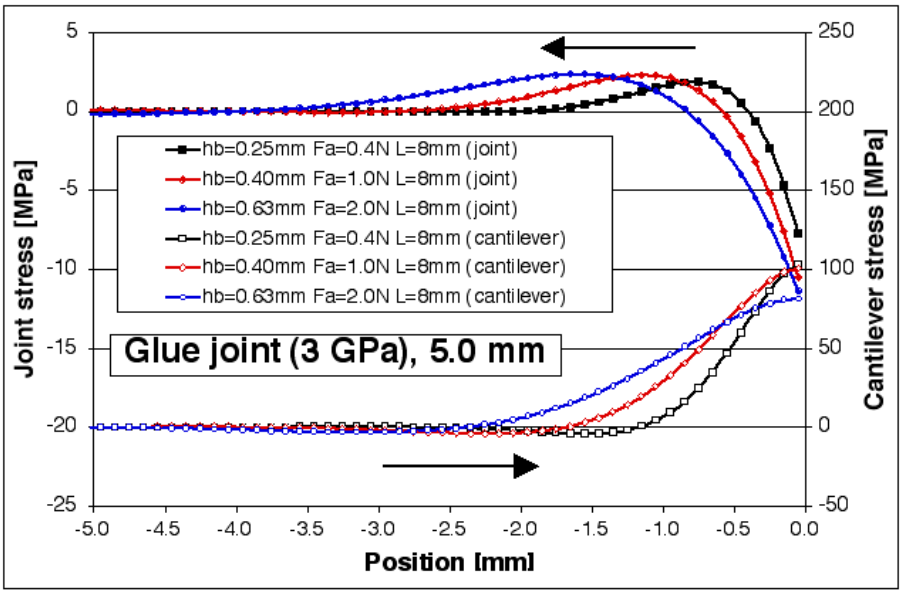

Figure 6. Stresses in cantilever & joint calculated by FD for 5.0 mm long glue joints.

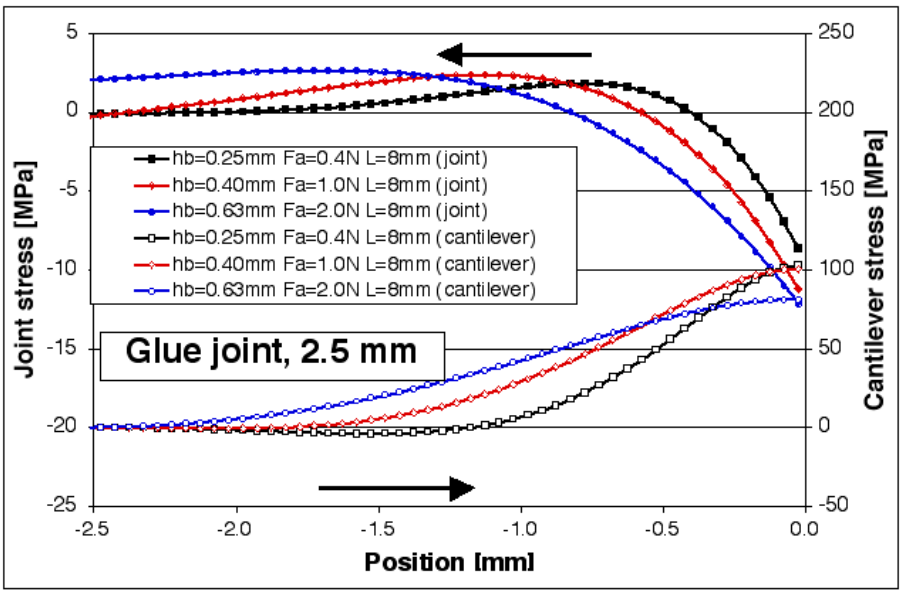

Figure 7. Stresses in cantilever & joint calculated by FD for 2.5 mm long glue joints.

4.4. Effect of a 15 MPa yield stress in the solder

This section is similar to 4.2, with 2.5 mm solder joint length, except that a yield stress σ_e of 15 MPa is introduced. This should be very conservative for the interior of the joint, as clamping of the solder by the alumina substrates is expected to raise this value significantly[iii]. This will also be confirmed in 4.6. However, clamping is not active at the joint edges, and around pores in the joint, and one should therefore stay conservative in specifying joint strengths…

Parameters and results are given in table 5 and in figures 8 and 9. Fig. 8 gives stress distributions for the different MilliNewton ranges, and fig. 9 shows the effect of varying the solder joint length L_j for the highest force range – and hence the most critical one for the joint. Even for the 2 N range at the shortest joint length, the structural integrity of the joint is conserved. However, significant plastic deformation of the joint occurs, given by L_p in table 5. The maximum tensile stress is only little affected by plastic deformation, but a significant increase is observed for the 2 N range at 1.5 mm joint length, which is close to the length at which the joint would fail at 2 N (1.2 mm, see section 4.6).

Symbol	Description	Value (400)	Value (1'000)	Value (2'000)	
E_b	Cantilever effective elastic modulus	330	330	330	GPa
E_j	Joint elastic modulus	30	30	30	GPa
σ_e	Joint yield stress	15	15	15	MPa
h_b	Cantilever thickness	0.25	0.40	0.63	mm
h_j	Joint thickness	0.10	0.10	0.10	mm
L_j	Joint length (for finite difference method)	2.5	2.5	1.5 2.5 5.0	mm
L	Cantilever effective length	8.0	8.0	8.0	mm
b	Width of cantilever and of joint	3.0	3.0	3.0	mm
F_a	Applied bending force	0.4	1.0	2.0	N
σ_{jmax}	Maximum tensile stress in solder	5.8	7.0	8.5 7.2 7.1	MPa
L_p	Length of plastic deformation in joint	0.11	0.22	0.35	mm

Table 5. Parameters for the three force ranges of MilliNewton. Joint length is also varied for 2 N range.

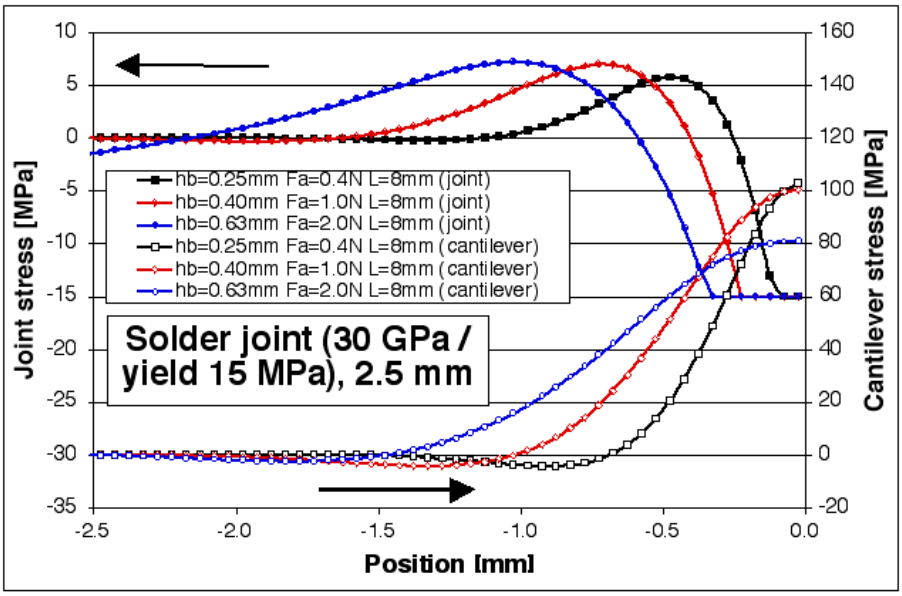

Figure 8. Stresses in cantilever & joint calculated by FD for 2.5 mm long solder joints with a yield stress of 15 MPa, for the different MilliNewton force ranges.

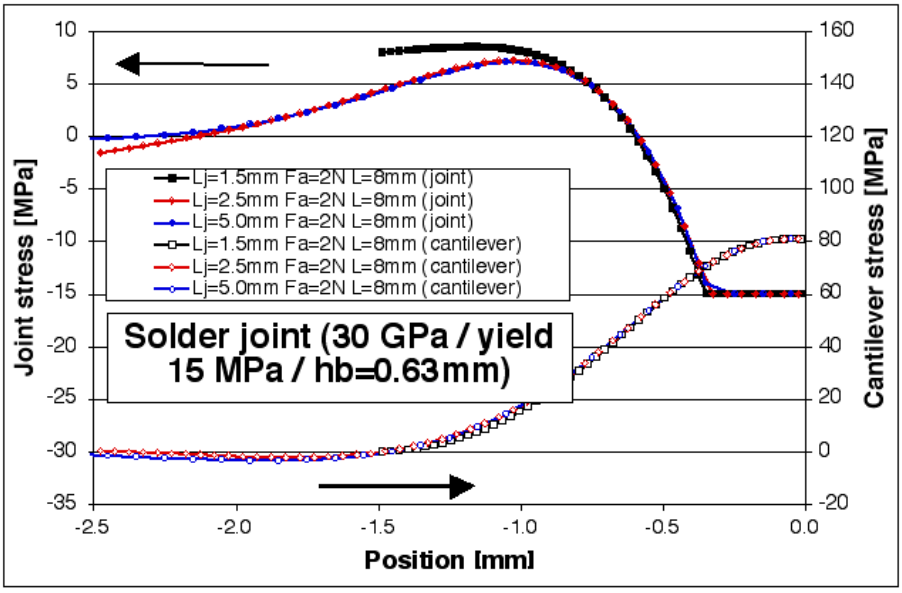

Figure 9. Stresses in cantilever & joint calculated by FD for solder joints of varying length, with the highest MilliNewton force range.

4.5. Varying the yield stress in the solder

In this section, the effect of varying the yield stress is explored, for the highest force range of MilliNewton. Parameters and results are given in table 6 and fig. 10.

Symbol	Description	Value (30 MPa)	Value (20 MPa)	Value (10 MPa)	
E_b	Cantilever effective elastic modulus	330	330	330	GPa
E_j	Joint elastic modulus	30	30	30	GPa
σ_e	Joint yield stress	30	20	10	MPa
h_b	Cantilever thickness	0.63	0.63	0.63	mm
h_j	Joint thickness	0.10	0.10	0.10	mm
L_j	Joint length (for finite difference method)	2.5	2.5	2.5	mm
L	Cantilever effective length	8.0	8.0	8.0	mm
b	Width of cantilever and of joint	3.0	3.0	3.0	mm
F_a	Applied bending force	2.0	2.0	2.0	N
σ_{jmax}	Maximum tensile stress in solder	7.4	7.3	6.8	MPa
L_p	Length of plastic deformation in joint	0.07	0.18	0.55	mm

Table 6. Parameters for the highest force range of MilliNewton – varying yield stress.

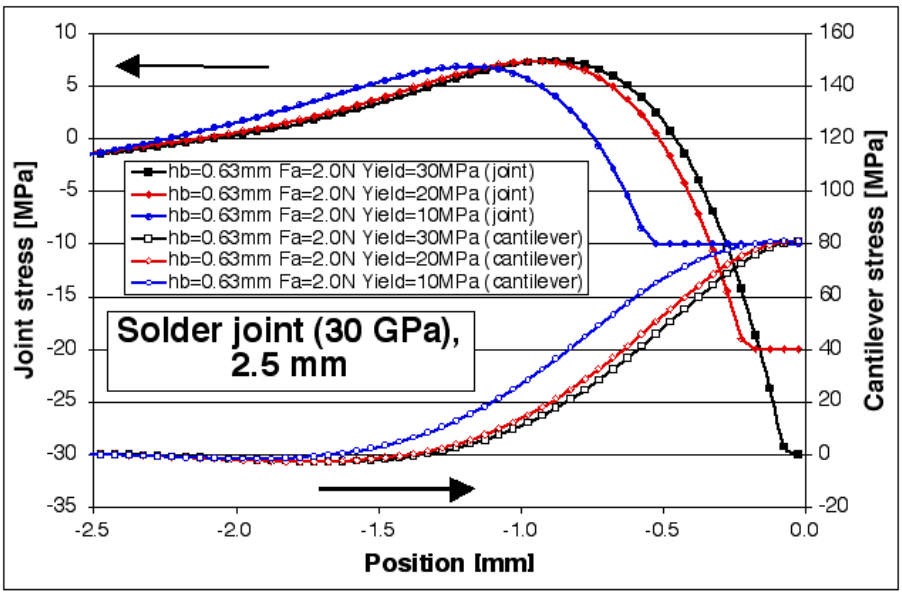

Figure 10. Stresses in cantilever & joint calculated by FD for 2.5 mm long solder joints and the highest MilliNewton force range, with varying yield stress.

4.6. Tests of solder strength

In 1999, Sven Stauss[i] conducted 3–point bending tests on Sn–Ag and Sn–Pb–Ag solder joints on thick (1.5 mm) alumina beams. The joints had the same widths as the beams, and lengths of 1, 2 and 4 mm. Surprisingly, only the 1 mm long joints gave results on the solder, as the alumina beams broke before joint failure for the other lengths.

Although there was some variation in joint failure stress as a function of solder material and geometry, most results fell within a ±30% range. Typical values are given below in table 7.

One can extract a rough estimation of the solder strength by assuming purely plastic deformation (fig. 2, no work hardening or striction) in all the joint, e.g. $\sigma_j = +\sigma_e$ for $-L_j < x < -u$ and $\sigma_j = -\sigma_e$ for $-u < x < 0$. If the lever arm L is long compared to the joint length L_j, one can neglect the effect of the applied force F_a on u and treat the case as a pure applied moment $F_a \cdot L$.

$$(30) \quad u = \frac{L_j}{2} + \frac{F_a}{2\sigma_e \cdot b} \cong \frac{L_j}{2}$$

$$(31) \quad F_a \cdot L = \frac{\sigma_e \cdot b}{2}\left(L_j^2 - 2u^2\right) \cong \frac{1}{4}\sigma_e \cdot b \cdot L_j^2$$

$$(32) \quad \sigma_e \cong \frac{4F_a \cdot L}{b \cdot L_j^2}$$

Parameters and results are given in table 7. From equation (32), the strength of the solder in the joint is >70 MPa. Even for very slow tests (rupture in ca. 30 min), rupture for sound 2 mm samples occurred in the beam.

The actual stress must be much higher at the end of the joint, as seen when comparing 2 mm and 4 mm long joints. Although rupture occurred in both cases in the beam, the nominal beam stress at rupture is much smaller for 2 mm. Therefore, considerable stress concentrations must occur at the end of the solder joint, which is expected as the cantilever beam thickness is comparable to the length of the joint, and means that the actual strength of the solder is probably much higher than 70 MPa. A precise estimation falls outside the scope of this work, and will be the subject of finite element modelling (FEM) studies.

However, we can attempt, to compare, as in the cantilever case treated in previous sections, the characteristic length L_c to the joint length. In our case, we get $L_c \cong 0.89$ mm, which means that stresses are not fully degraded over 2 mm, especially if some plastic deformation occurs at the edges. A rough estimation of joint edge stresses was attempted by superposing the effect of two cantilevers, one on each side of the joint, loaded with $\pm F_a$ (since we have two cantilevers instead of one cantilever and a base), which gives a stress of $\sigma_j(0) - \sigma_j(-L_j)$.

Although these calculated joint stresses are certainly incorrect because of the very approximate model and the fact that some plastic deformation must be occurring at the edges, we clearly see that the stress in the joint increases much less than the bending moment / the nominal cantilever stress. Therefore, this rough estimation shows that increasing the joint length decreases the stress concentration, and thereby qualitatively explains the apparent increase of cantilever bending strength when going from 2 mm to 4 mm joint length.

Symbol	Description	Value (1 mm)	Value (2 mm)	Value (4 mm)	
L_j	Joint length	1.0	2.0	4.0	mm
h_b	Cantilever thickness	1.5	1.5	1.5	mm
h_j	Joint thickness (ca.)	0.05	0.05	0.05	mm
E_b	Cantilever effective elastic modulus	330	330	330	GPa
E_j	Joint elastic modulus	30	30	30	GPa
L	Cantilever effective length	19.5	19.0	18.0	mm
b	Width of cantilever and of joint	10.7	10.7	10.7	mm
F_a	Typ. force at rupture / 2 (3-pt bending)	10	40	75	N
σ_e	Joint yield stress from equation (32)	73	>71	>32	MPa
$\sigma_j(0) - \sigma_j(-L_j)$	Stress at joint edge (FD), if elastic	(232)	272	348	MPa
σ_b	Cantilever nominal stress at rupture	49	189	336	MPa
	Rupture mode	joint	beam	beam	

Table 7. Parameters and results for solder strength tests[i].

4.7. A small note on membranes made by glass sealing

Glass seals are seldom used in cantilever structures due to their excessive brittleness. They are however very useful for assembled pressure sensors where the membrane geometry is defined by the glass seal. Under some assumptions (membrane size $>> L_c$, thickness), we can transpose the calculations in this work to the membrane case, as, the joint locally undergoes the same type of loading (a force and a bending moment).

In this section, we assume a round alumina membrane of D = 10 mm diameter, h_b = 0.12, 0.17 or 0.25 mm thickness, loaded with ΔP = 1 bar differential pressure (about 1.4 bar absolute assuming 0.4 bar internal pressure), and sealed by a soft solder glass (E_j = 50 GPa, h_j = 50 μm). The force F_a applied on the membrane – and carried by the joint – is given by:

$$(33) \quad F_a = \frac{\pi \cdot D^2}{4} \cdot \Delta P$$

The following expression gives the radial bending stress at the edge[iv], equivalent to the nominal cantilever stress. In order to adapt the membrane case to our model, we must also express it in terms of cantilever parameters L and b:

$$(34) \quad \sigma_b = \frac{3D^2}{16h_b^2} \cdot \Delta P = \frac{6L}{b \cdot h_b^2} \cdot F_a, \text{ where } b = \pi \cdot D \text{ and } L = \frac{D}{8}$$

The width b is simply the perimeter of the membrane. The length L is calculated to give the same stress, by substituting (33) into (34).

The parameters and calculated results are given for the three thicknesses in table 8. For the thinnest membranes, one should somewhat reduce the membrane diameter in order to reduce the nominal stress to less than 100 MPa. As glass seals give a comparatively thin and stiff joint, the characteristic length L_c is very small – and the joint stresses quite high. In our case, a sound 1 mm wide seal is amply sufficient to ensure complete stress decay for such thin membranes.

Symbol	Description	Value (0.12)	Value (0.17)	Value (0.25)	
E_b	Cantilever effective elastic modulus	330	330	330	GPa
E_j	Joint elastic modulus	50	50	50	GPa
ΔP	Differential pressure on membrane	0.1	0.1	0.1	MPa
h_b	Membrane thickness	0.12	0.17	0.25	mm
h_j	Joint thickness	0.05	0.05	0.05	mm
D	Membrane diameter	10.0	10.0	10.0	mm
b	Equivalent width of cantilever and of joint	31.4	31.4	31.4	mm
L	Equivalent cantilever effective length	1.25	1.25	1.25	mm
F_a	Applied bending force	7.9	7.9	7.9	N
L_c	Calculated caracteristic length	0.12	0.15	0.20	mm
σ_b	Nominal stress at membrane edge (radial)	130	65	30	MPa
σ_{j0}	Calculated stress in joint at x=0	-50	–30	–18	MPa
σ_{jmax}	Maximum tensile stress in joint	9.4	5.6	3.2	MPa

Table 8. Parameters for low-presure sensors assembled by glass sealing.

5. Discussions and conclusions

The concept of the characteristic length L_c for the decay of the stresses is very useful in determining the minimal joint length L_j. From our results, we see that we should have about $L_j \geq 3 \cdot L_c$ to minimise the stresses in the joint. This condition is satisfied for the MilliNewton sensors. Note that our model only gives an approximate estimation of Lc, because the condition $L_c >> h_b$ is not satisfied.

A change from solder to conductive glue leads to a much more compliant joint, and gives rise to an increase of L_c, thereby requiring longer joints in theory. However, this apparent disadvantage is more than offset by the considerably lower stresses in the joint – the load on the cantilever is spread over a much greater length if the joint material has a lower modulus. Additionally, epoxy glue is less prone to plastic deformation than solder, and the lower modulus also means lower parasitic stresses in the cantilever, leading to lower drift in theory.

Aside from the material, the rigidity of the joint can also be changed through its thickness – actually, the ratio E_j / h_j is the determining factor.

One argument speaking against conductive glue is its poor performance in hot and humid environments (85 C / 85% RH)[v], which is due to corrosion of the silver. However, this should not be a problem under more moderate conditions. For instance, no problem was observed for 170 h in ambient air heated at 100 C. Furthermore, creep of conductive glue was found to be considerably less than that of both Sn–Ag and Sn–Pb–Ag solder[v]. In fact, long-term reliability of solder under creep and fatigue is problematic[vi] [vii], and is probably the most worrisome issue facing soldered cantilevers. In any case, harder solders such as Sn–Ag (Sn96), Sn–Cu–Ag and Sn–Sb (Sb5) should be preferred over Sn–Pb (Sn63) or the somewhat better Sn–Pb–Ag (Sn62). One should however be careful not to extract hasty conclusions, as the solder joint between two hard alumina surfaces behaves differently from the bulk material: a strengthening effect is observed in practice (section 4.6).

Long-term reliability of glass seals is limited by a phenomenon called static fatigue[viii] [ix]. However, a cyclic fatigue effect is low or inexistent. In standard glass, a tensile stress of 10 MPa is considered safe, although this depends on environment: static fatigue is actually a kind of stress corrosion, the most common cause being ambient humidity. This means that higher tensile stresses may be sustained provided they are insulated from the environment. This is the case for a good glass seal (section 4.7): the zone in tension is sealed away from the ambient air, although one cannot say if this can be garanteed, due to possible porosity in the joint. This is easier to obtain in an absolute sensor, where the whole inner volume is sealed away from the ambient provided the seal is hermetic.

Bibliography

[i] Stauss-S, "Assemblage de substrats pour circuits hybrides par brasage", Projet de semestre EPFL-LPM, 1999.

[ii] Krasnov-ML Kiselyov-AI Makarenko-GI, "A book of problems in ordinary differential equations", Ed. Mir, Moscow , 1981.

[iii] Olson-DLR Siewert-TA Liu-S Edwards-GR, "ASM Handbook vol. 6: Welding, Brazing and Soldering", ASM International, 1991.

[iv] Maeder–T, "Capteurs piézorésistifs à couches épaisses - bases de calcul", chapter 6, EPFL–LPM report, preliminary, 2000.

[v] Maeder-T Genoud-D, "Solder assembly of cantilever bar force or displacement sensors", Sensor 2001, Nürnberg, Germany, 2001.

[vi] Vianco-PT, "ASM Handbook vol. 6: Welding, Brazing and Soldering - General Soldering", ASM International 6, 965-984, 1991.

[vii] Weber-L, "Creep and fatigue behaviour of eutectic Sn62Pb36Ag2", ETHZ thesis no. 12251, 1992.

[viii] Gy-R, "Stress corrosion of silicate glass: a review", Journal of Non-Crystalline Solids 316, 1-11, 2003.

[ix] Lü-BT, "Fatigue strength prediction of soda-lime glass", Theoretical and Applied Fracture Mechanics 27, 107-114, 1997.